Available online at http://www.ijasrd.org/in

International Journal of Advanced Scientific Research & Development
Vol. 02, Iss. 01, Ver. I, Jan – Mar’ 2015, pp. 87 – 100

e-ISSN: 2395-6089
p-ISSN: 2394-8906

DESIGN AND IMPLEMENTATION OF TRANSFORMERLESS INVERTER WITH DC CURRENT ELIMINATION

R. Manivannan
Assistant Professor, Department of Electrical and Electronics Engineering, Christ College of Engineering and Technology, Puducherry, India.

N. Thirumurugan
PG Student, Department of Electrical and Electronics Engineering, Christ College of Engineering and Technology, Puducherry, India.

Dr. T. S. Sivakumaran
Professor, PG Dean, Arunai Engineering College, Thiruvannalamalai.

ARTICLE INFO

Article History:
Received: 23 Mar 2015;
Received in revised form: 25 Mar 2015;
Accepted: 25 Mar 2015;
Published online: 31 Mar 2015.

Key words:
Basic Mode (CM) Present,
Photovoltaic (PV) Framework,
Exchanged Capacitor,
Transformer Less Inverter,
Unipolar Sinusoidal Heartbeat Width Tweak (SPWM),
Virtual DC Transport.

ABSTRACT

In order to eliminate the normal mode spillage current in the transformer less photovoltaic framework. By joining the framework impartial line specifically to the negative shaft of the dc transport, the stray capacitance between the PV boards and the ground is skirted. Thus, the CM ground spillage current can be stifled totally. It comprises of just five switches, two capacitors, and a solitary channel inductor. Accordingly, the force gadgets expense can be curtailed. This propelled topology can be balanced with the unipolar sinusoidal heartbeat width balance (SPWM) and the twofold recurrence SPWM TO decrease the current swell.

Copyright © 2015 IJASRD. This is an open access article distributed under the Creative Common Attibution License, which permits unrestricted use, distribution, and reproduction in any medium, provided the original work is properly cited.

INTRODUCTION

This Paper Proposes a framework taking into account the mix of Cockcroft-Walton (CW) voltage multiplier and the transformer less Photovoltaic (PV) Virtual DC transport module. Furnishing nonstop include current with low swell, high voltage degree, and low voltage weight on the switches, diodes, and capacitors, the proposed converter is truly suitable for applying to low-enter level dc era frameworks. In addition, taking into account then-organize CW voltage multiplier, the proposed converter can give a suitable dc source to a n+1-level multilevel inverter. In this paper the framework mixture of PV, virtual DC transport and CW voltage multiplier with low swell, high voltage proportion is proposed. The idea of the virtual dc transport is taking out the basic mode (CM) spillage current in

How to cite this article: Manivannan, R., Thirumurugan, N., & Sivakumaran, T. S., (2015). “Design and Implementation of Transformerless Inverter with DC Current Elimination”. *International Journal of Advanced Scientific Research & Development (IJASRD), 02* (01/I), pp. 87 – 100.

the transformer less photovoltaic (PV) frameworks. The yield of the transformer less inverter with virtual DC transport is joined with data of the Cockcroft Walton voltage multiplier. It proposes a high venture up dc-dc converter in light of the Cockcroft-Walton (CW) voltage multiplier without a stage up transformer. The proposed control system utilizes two free frequencies, one of which works at high recurrence to minimize the extent of the inductor while the other one works at generally low recurrence as per the sought yield voltage swell.

Fig. 1: *CM current path for the transformerless PV inverter.*

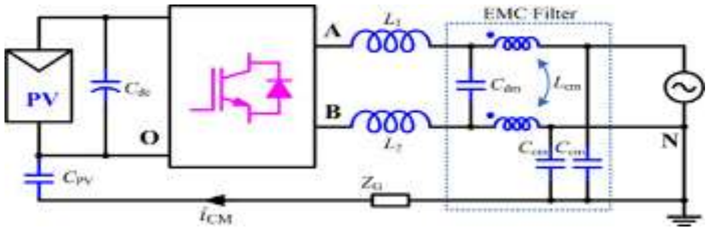

Fig. 2: *Equivalent circuit for the CM current path.*

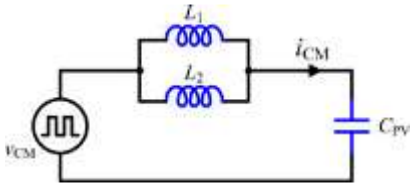

In the customary lattice joined PV inverters, either a line- recurrence or a high-recurrence transformer is used to give a galvanic seclusion between the framework and the PV boards. Re- moving the segregation transformer can be a powerful answer for increment the effectiveness and lessen the size and expense[6]. How- ever, if the transformer is excluded, the regular mode (CM) ground spillage current may show up on the parasitic capacitor between the PV boards and the ground[7][8]. The presence of the CM current may diminish the force change productivity, expand the network current bending, crumble the electric magnetic similarity, and all the more essentially, offer ascent to the security dangers[9].

The CM current way in the matrix joined transformer less PV inverter framework is shown in Fig. 1. It is shaped by the force switches, channels, ground impedance ZG, and the parasitic capacitance CPV between the PV boards and the ground. As indicated by[10], the CM current way is proportional to a LC resounding circuit in arrangement with the CM voltage, as demonstrated in Fig. 2. The CM voltage vCM is characterized

$$v_{\mathrm{CM}} = \frac{v_{\mathrm{AO}} + v_{\mathrm{BO}}}{2} + (v_{\mathrm{AO}} - v_{\mathrm{BO}})\frac{L_2 - L_1}{2(L_1 + L_2)}$$

where vAO is the voltage contrast between focuses An and O, vBO is the voltage distinction between focuses B and O, and L1 and L2 are the yield channel inductors If the exchanging activity of the inverter produces high- recurrence CM voltage, the CM current iCM may be left on the LC circuit. Starting here of perspective, the topology and tweak system received for the transformer less PV power framework ought to ensure that vCM is steady or just changes at low recurrence, for example, 50 Hz/60 Hz line recurrence.

A straightforward approach to understand this objective is to utilize the full-connect inverter with the bipolar sinusoidal heartbeat width regulation (SPWM), of which the CM voltage is altered at a large portion of the dc transport volt- age. Contrasting and the bipolar SPWM, the unipolar SPWM has better execution as far as the yield current swell and exchanging misfortunes, yet can't be straightforwardly utilized for the full-connect inverter in the transformer less application, on the grounds that it produces the exchanging recurrence CM voltage.

Consequently, some best in class topologies, for example, the H5 inverter, the HERIC inverter, and so on., have been created taking into account the full-connect inverter, to keep vCM steady when the unipolar balance is utilized[11]–[16]. Some of these topologies are shown in Fig. 3. By embeddings additional switches into the full- span inverter either on the dc or air conditioning side, the dc transport can be separated from the lattice when the inverter yield voltage is at zero voltage level, so that the CM current way is cut off. Such arrangements require two channel inductors with autonomous iron centers, which may rompt an ascent in the size and expense. Additionally, the dc and air conditioning sides can't be superbly detached by the force switch due to the switch parasitic capacitance, so the CM current may even now exist[10].

An alternate sort of arrangement is to utilize the half-connect inverter with the framework nonpartisan line straightforwardly associated with the midpoint of the dc transport, as indicated in Fig. 4. Along these lines, the voltage over the parasitic capacitor is clipped to be steady by the dc transport capacitor. In any case, this technique has an imperative weakness that the obliged dc transport voltage ought to be multiplied contrasted and the full-connect topologies. For the 220 Vac framework, it can be as high as 700 V.

Despite the fact that the three-level nonpartisan point cinched (NPC) circuit can help enhance the execution of the half-connect inverter, the dc transport voltage is still high[17][18]. Other than the previously stated exemplary circuits, there are different topologies proposed in late writing works, some of which are recorded in Fig. 5. The Karschny inverter[19] and the paralleled- buck inverter[20] are gotten from the buck–boost and buck circuits, separately. These arrangements have high dependability, however are not fit for supplying the responsive energy to the lattice.

Fig. 3. *Full-extension based topologies for the transformerless inverter: (a) H5 circuit* [11]*; (b) HERIC circuit* [12]*; (c) H6 circuit with air conditioning detour* [13]*; (d) H6 circuit with dc sidestep* [15].

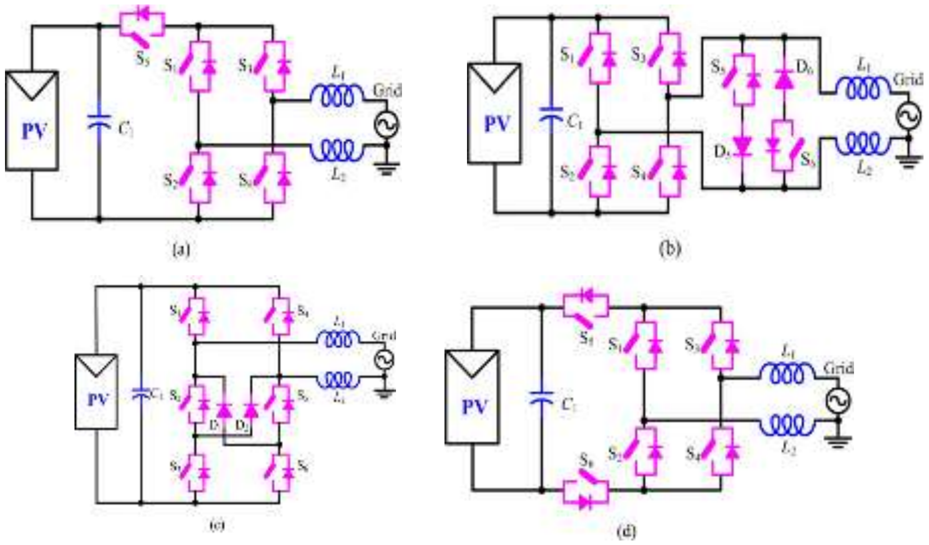

The inverter proposed in[21] utilizes a capacitor voltage divider to keep the CM voltage consistent, yet is respected to be of higher conduction misfortunes. In this paper, a novel topology era system called the virtual dc transport idea is proposed for the transformer less framework associated PV inverter. In this arrangement, the framework unbiased line is joined straightforwardly to the negative shaft of the dc transport, so that the voltage over the parasitic capacitor is clasped to zero. Accordingly, the CM current is wiped out totally. In the interim, the virtual dc transport is made to help create the negative yield voltage. The obliged dc transport voltage is still the same as the full-connect, and there is not any restriction on the tweak technique since the CM current is evacuated regularly by the circuit structure thusly, the focal points of the full-connect and half-scaffold based arrangements are consolidated together.

Fig. 4. *Half-Scaffold Based Topologies. (a) Routine Half-Connect Inverter. (b) NPC Half-Connect Inverter*

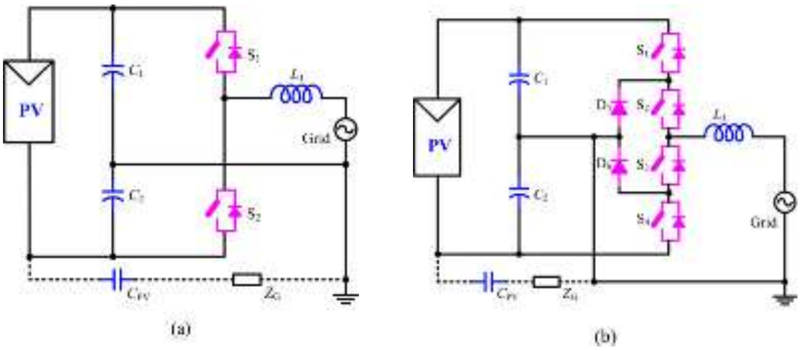

(a)

(b)

Fig. 5. *Other Transformerless Inverter Topologies: (a) Karschny Inverter*[19]*; (b) Paralleled-Buck Inverter*[20]*; (c) H6 Inverter with Capacitor Voltage Divider*[21]*.*

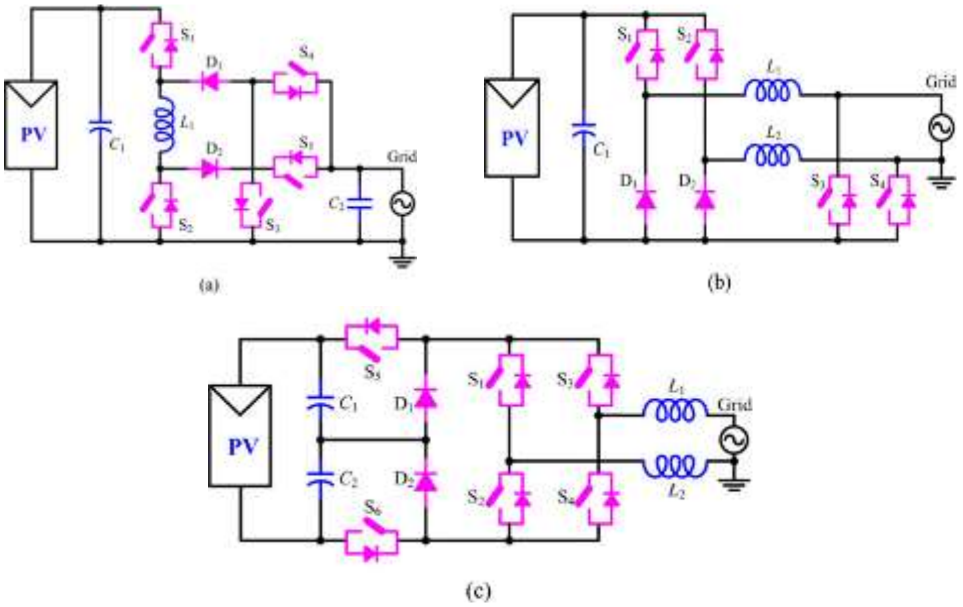

(a)

(b)

(c)

Taking into account the previously stated imaginative thought, a novel inverter topology is proposed with the virtual dc transport idea by utilizing the exchanged capacitor innovation. The proposed inverter can be adjusted with the unipolar SPWM and twofold recurrence SPWM. It comprises of just five force switches and a solitary channel inductor, so the expense of the semiconductor and attractive segments can be diminished. This paper is sorted out as takes after. The virtual dc transport idea is clarified in Area II. Taking into account it, a novel inverter topology with the exchanged capacitor is determined in Area III, and the balance method and operation rule are depicted in subtle element. The current anxiety created by the operation of the exchanged capacitor is broke down in Area IV. The circuit execution is assessed in Area V. The test consequences of a 500-W model with 20 kHz exchanging recurrence are given in Area VI to check the examination. A synopsis is given in the last segment.

1.1 Virtual DC Transport Idea

The idea of the virtual dc transport is delineated in Fig. 6. By joining the framework nonpartisan line straightforwardly to the negative shaft of the PV board, the voltage over the parasitic capacitance CPV is cinched to zero. This keeps any spillage current coursing through it.

As for the ground point N, the voltage at midpoint B is either zero or +Vdc, as per the condition of the switch span. The reason for presenting the virtual dc transport is to produce the negative yield voltage, which is important for the operation of the inverter. In the event that a fitting system is intended to exchange the vitality between the genuine transport and the virtual transport, the voltage over the virtual transport can be kept the same as the genuine one. As indicated in Fig. 6, the positive shaft of the virtual transport is associated with the ground point N, so that the voltage at the midpoint C is either zero or −Vdc. The specked line in the figure demonstrates that this association may be acknowledged specifically by a wire or by implication by force switch. With focuses B and C joined together by a brilliant selecting switch, the voltage at point A can be of three diverse voltage levels, in particular +Vdc , zero, and −Vdc .

Since the CM current is disposed of commonly by the structure of the circuit, there is not any confinement on the regulation strategy, which implies that the propelled balance advances, for example, the unipolar SPWM or the twofold recurrence SPWM can be utilized to fulfill different PV application

INFERRED TOPOLOGY AND ADJUSTMENT METHODOLOGY

In light of the virtual dc transport idea, a novel inverter topology is determined as a sample to demonstrate the agreeable focal points of the proposed procedure, which is demonstrated in Fig. 7. It comprises of five force switches S1 – S5 and stand out single channel inductor Lf. The PV boards and capacitor C1 structure the genuine dc transport while the virtual dc transport is given by C2. With the exchanged capacitor innovation, C2 is charged by the genuine dc transport through S1 and S3 to keep up a steady voltage. This topology can be balanced with the unipolar SPWM and twofold recurrence SPWM. The nitty gritty examination is presented as takes after.

Fig. 6: *Virtual DC Bus Concept*

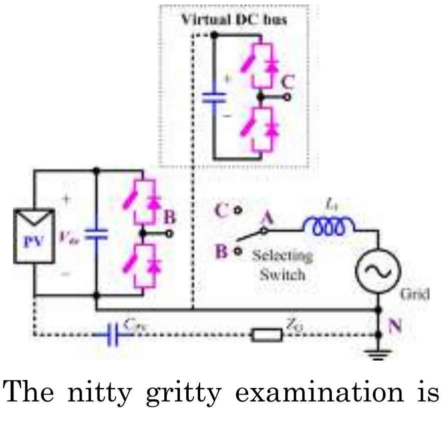

Fig. 7: *Proposed Topology*

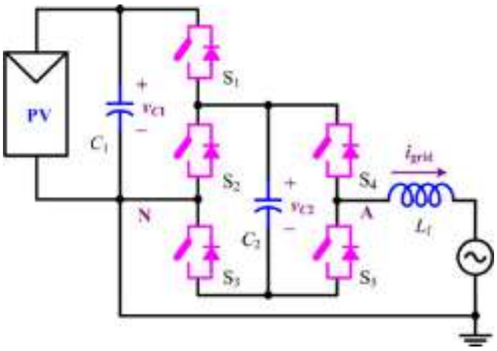

Fig. 8: *Unipolar SPWM for the Proposed Topology*

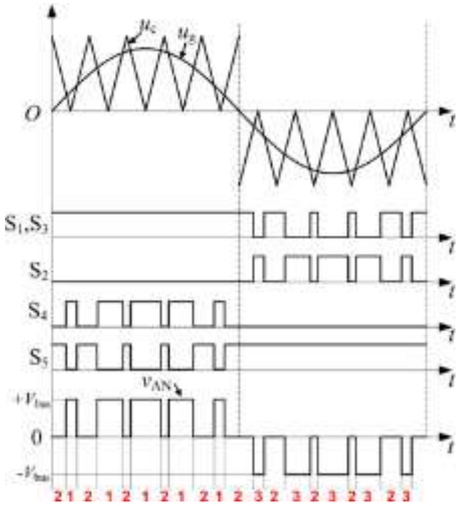

2.1 Unipolar SPWM

The waveform for the unipolar SPWM of the proposed inverter is shown in Fig. 8. The door drive signals for the force switches are created by relative estimation of the regulation wave ug and the bearer wave uc. Half network cycle, ug > 0. S1 and S3 are turned ON and S2 is killed, while S4 and S5 commutate complementally with the autorier recurrence. The capacitors C1 and C2 are in parallel and the circuit turns between states 1 and 2 as indicated in Fig. 10.

Fig. 9: *Double-Frequency SPWM for the Proposed Topology*

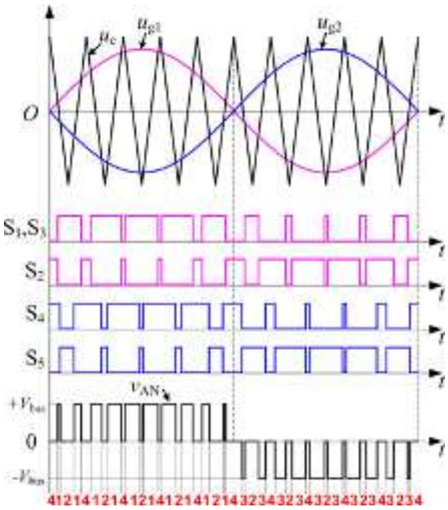

Amid the negative half cycle, ug < 0. S5 is turned ON and S4 is killed. S1 and S3 commutate with the bearer recurrence synchronously and S2 commutates in supplement to them. The circuit turns between states 3 and 2. At express 3, S1 and S3 are killed while S2 is turned ON. The negative voltage is created by the virtual dc transport C2 and the inverter yield is at negative voltage level. At express 2, S1 and S3 are turned ON while S2 is killed. The inverter yield voltage vAN equivalents zero; in the meantime, C2 is charged by the dc transport through S1 and S3. B. Twofold Recurrence SPWM

The proposed topology can likewise work with twofold recurrence SPWM to attain to a higher identical exchanging recurrence, as indicated in Fig. 9. In the twofold recurrence SPWM, the five force switches are differentiated into two sections, and are modulated with two backwards sinusoidal waves individually. S1, S2, and S3 are adjusted with ug1, while S4 and S5 are balanced with ug2. Amid the positive half framework cycle, the circuit pivots in the arrangement of "state 4 – state 1 – state 2 – state 1," and the yield voltage vAN differs between +Vdc and the zero with twice of the transporter recurrence.

Fig. 10: *Equivalent Circuits for States 2 and 3: (a) State 2; (b) State 3*

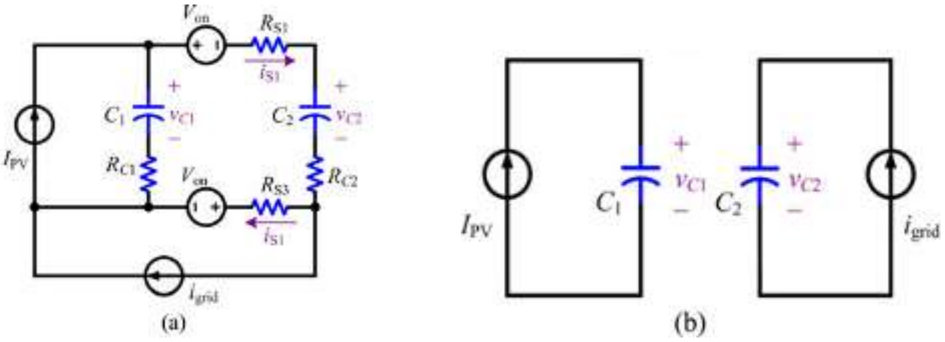

For the majority of the four operation states, there is no impediment on the heading of the yield current grid, since the force switches with antiparallel diodes can accomplish bidirectional current stream. Accordingly, the proposed topology has the ability of bolstering responsive force into the lattice to help bolster the strength of the force framework.

The proposed topology is additionally invulnerable against transient over- voltage of the matrix. Amid the mains positive voltage spikes, the voltage at point An is clasped at Vdc by C1 and the antiparallel diodes of S1 and S4. Additionally, amid the negative voltage spikes, the voltage at point An is clasped at −Vdc by C2 and the antiparallel diodes of S2 and S5. Along these lines, the mains transient overvoltage does not represent a security risk for the inverter.

2.2 Current Anxiety Investigation

One imperative normal for the proposed topology is the use of the exchanged capacitor innovation. The operation of the exchanged capacitor may apply some additional current weight on the force switches, which lessens the proficiency and builds the current weight on the gadgets. It is important to cutoff this current to a worthy quality to guarantee the dependability of the inverter. In this segment, the current anxiety is examined quantitatively with outline rules gave. The investigation beneath is in light of the unipolar SPWM and unit yield force component.

2.3 Exchanging Misfortunes

Amid the positive half cycle, just two switches, in particular S4 and S5, commutate at the bearer recurrence, so the exchanging misfortunes are the same as the customary full-connect inverter. Amid the negative half cycle, S1, S2, and S3 commutate at the bearer recurrence. Despite the fact that the quantity of high-recurrence switches increments to 3, it can be seen from the accompanying examination that the exchanging misfortunes just about keep the same.

For comfort of depiction, the force transistor and the antiparallel diode for the switch Sn is indicated as Tn and Dn separately, where n = 1, 2. . . 5.

At express 2, T1, T3, and T5 are turned ON, while the current really moves through T1, D3, and T5, as demonstrated in Fig. 13(a). At the point when the circuit changes from state 2 to express 3, T1 and T3 are killed first before T2 is turned ON because of the impact of the dead time. Therefore, there will be a move state between the two states, as demonstrated in Fig. 13(c). Amid this move express, the inductor Lf freewheels through D3, so the voltage crosswise over T1 and T3 may not rise promptly after killed, so that the exchanging misfortunes can be disregarded. At the point when the dead time is passed, T2 is turned ON. The inductor current is compelled to commutate from D3 to T2, and the circuit changes into state 3. At the point when the circuit pivots from state 3 to express 2, it likewise enters the move state first. Due to the dead time, T2 is killed while T1 and T3 are not turned ON yet, and the inductor current is compelled to commutate from T2 to D3. After D3 is leading, the voltage crosswise over S1 and S3 diminishes to zero give or take. In this way, when T1 and T3 are turned ON after the move state, they won't endure noteworthy exchanging misfortunes.

In synopsis, just T2 and D3 work in the constrained recompense mode amid the negative half cycle, and the voltage and current commutated are Vdc and igrid, separately. Thusly, the operation of the exchanged capacitor does not result in the increment in exchanging misfortunes. The quantity of constrained compensations for the diodes and transistors in a solitary exchanging cycle is outlined in Table I.

Comparative examination can be performed on the H5 circuit also, and the outcome is recorded in Table II. It can be seen that the quantity of constrained substitution for the transistors is multiplied for the H5 circuit, while the replacement voltage decreases to Vdc/2, so the resultant exchanging misfortunes can be thought to be at the same level.

Fig.11: *Current Path During Commutation:(a) State 2; (b) State 3; (c) Transition State Between 2 and 3*

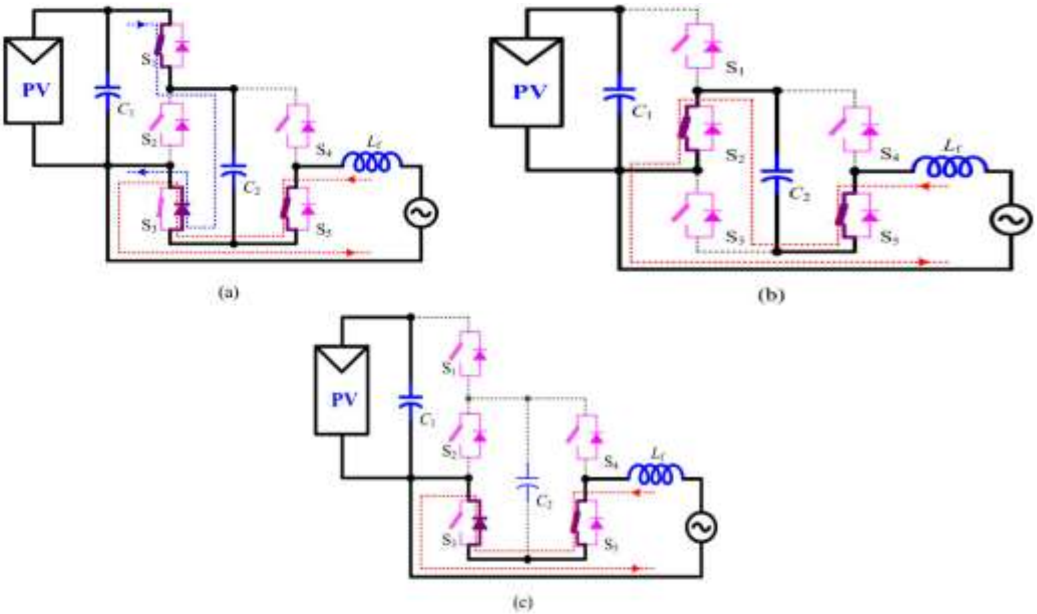

Table 1: *Summary of Forced Commutations for the Proposed Topology*

Device	Forced Commutation Number	Voltage	Current
Diode	2	V_{dc}	i_{grid}
Transistor	2	V_{dc}	i_{grid}

Table2: *Summary of Forced Commutations for the H5 Circuit*

Device	Forced Commutation Number	Voltage	Current
Diode	2	V_{dc}	i_{grid}
Transistor	4	$V_{dc}/2$	i_{grid}

This section describes the tests or instruments used to collect data. It would be appropriate to describe any questionnaires that you used. For example, if you used the Marlowe-Crowne Social Desirability Scale in your research, you may say that the Marlowe-Crowne Social Desirability Scale (MCSD; Crowne & Marlowe, 1960) comprises 33 true-false items that measure social desirability. You would also provide the reader with information regarding the MCSD scores' reliability and validity. Do this for each and every measure used in the study. In the event that the purpose of your paper is to develop a new questionnaire, you may wish to describe reliability and validity in the Results section (see below). However, you would only do this for a scale-development project.

2.4 CM Current Disposal

As clarified already, the key point for the full-scaffold based arrangements, including H5 and HERIC, is to embed additional switches into the conventional full-connect inverter to detach the line side with the dc side, when the inverter yield voltage is at zero voltage level. Lamentably, this disengagement is inadequate on account of the parasitic capacitance on the force switches. Accordingly, high-recurrence CM current may in any case course through these capacitors. Hence, it is important to include additional channels into these topologies to assimilate this CM current. With respect to the proposed topology, the stray capacitance between the PV boards and the ground is specifically circumvent. Because of the design of the virtual dc transport, the CM current is killed totally.

All in all, the conduction and exchanging misfortunes in the influence gadgets of the proposed topology are truly like those of the H5 circuit. The fundamental disadvantage is that bigger capacitors are expected to decrease the ESR misfortunes in the capacitor and guarantee their life time. This issue can be mitigated by including a slight film capacitor in parallel to the aluminum electrolyte one to assimilate the high-recurrence throbbing current. Luckily, the acceptable preference of the proposed topology is that it has better execution in disposing of the CM current. The arrangement with virtual dc transport idea gives another thought to building up the transformerless inverter for the PV applications.

REPRODUCTION RESULTS AND WAVEFORM

A model was assembled to confirm the legitimacy of the proposed converter. The framework determinations and the waveform clarify in detail the operation of proposed DC-DC help converter with seven-stage Cockcroft Walton voltage multiplier. Parts of the model are condensed in table I and table II, separately. Also, Matlab/Simulink is connected to recreate the mathematic model and control methodology of the proposed converter. Some chose waveforms of the proposed converter at Vin=12V, and Vo=230V for both reproduction and analysis. A model with comparing rating was manufactured to check the legitimacy of the proposed converter. In addition, the MATLAB Simulink is connected to recreate the mathematic model and the control procedure of the proposed converter.

Fig 12: *Transformerless Inverter with Virtual DC Bus*

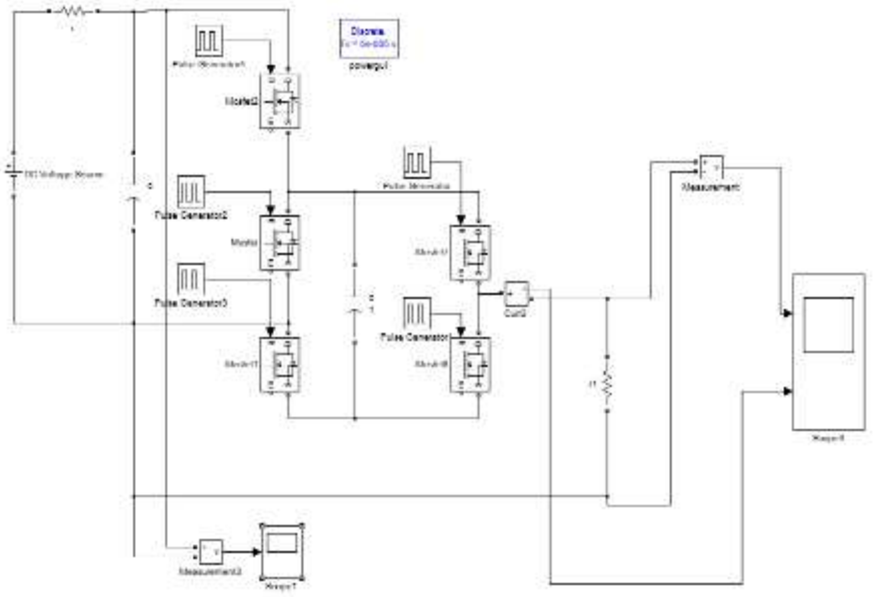

Fig 13: *Input of Transformerless Inverter*

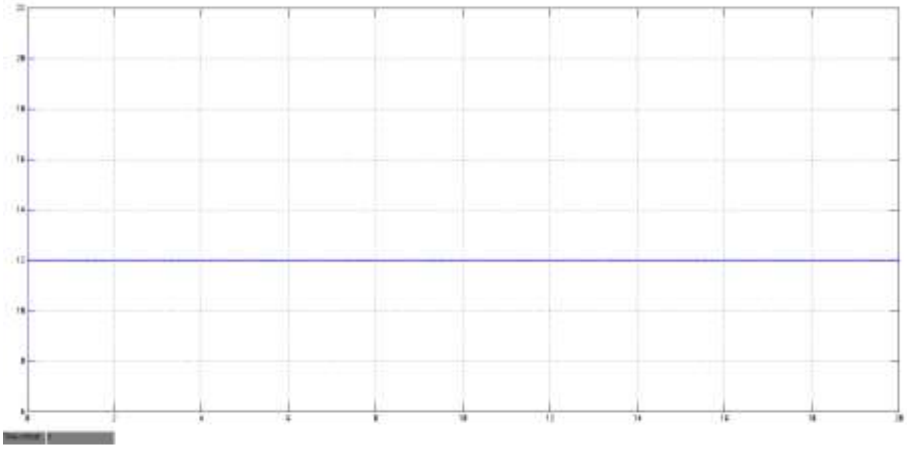

Fig 14: *Output of Transformerless Inverter with Virtual DC Bus*

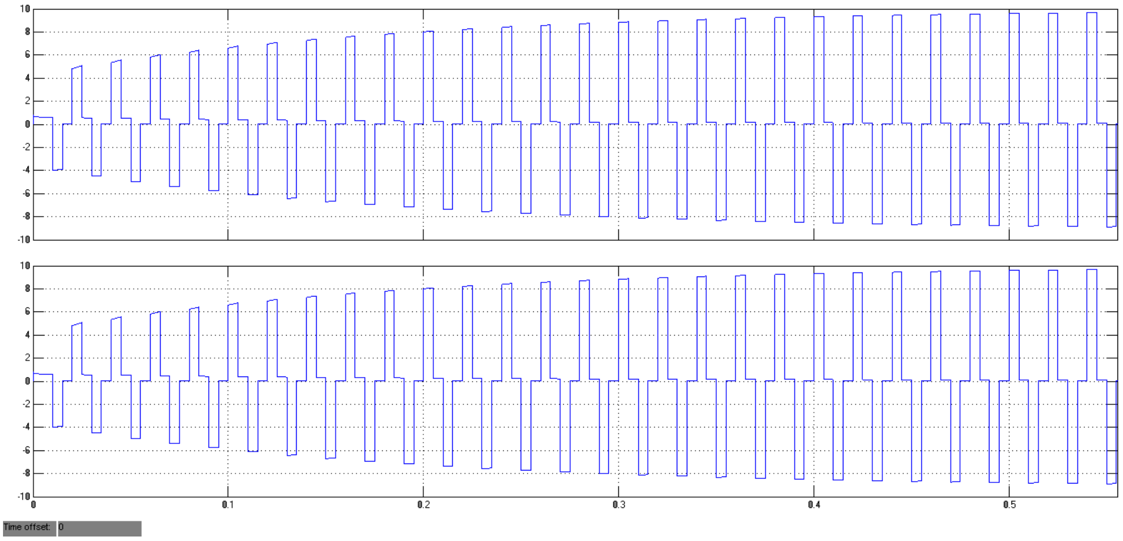

The recreation graph of Transformerless inverter with virtual DC transport is demonstrated in Fig.12. The reenactment of the data of Transformerless inverter is indicated in Fig.13. The reenactment yield waveform of Transformerless inverter with virtual DC transport is indicated in Fig.14.

Fig 15: *Output Wave Form of Proposed System Simulated Diagram*

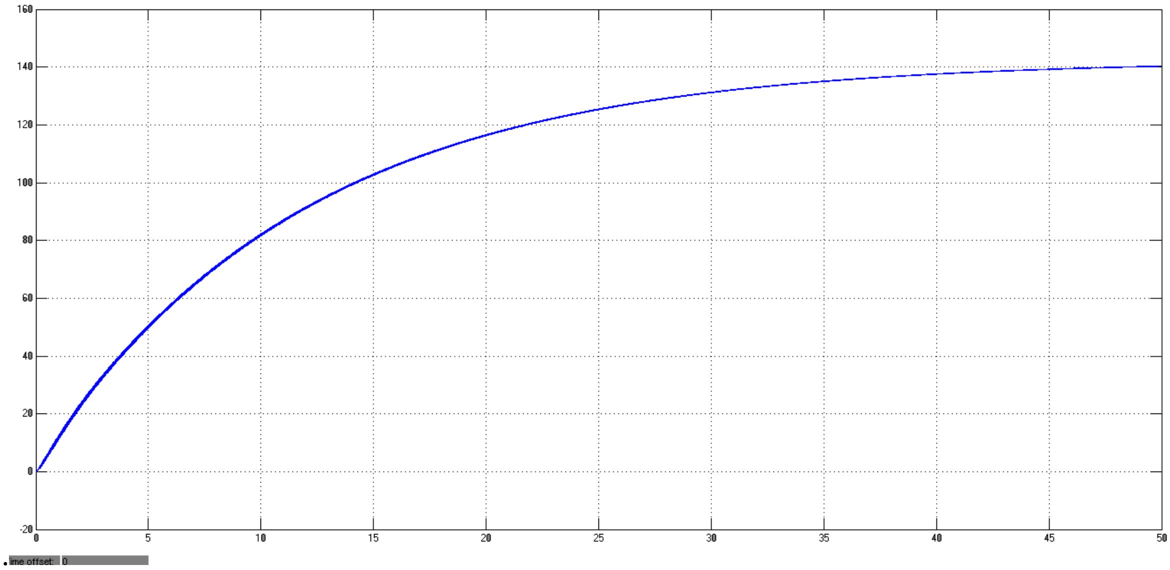

The outcomes speak to that the proposed converter has lower effectiveness at lower data in view of higher directing misfortune joined by higher information current. Then again, for higher burden condition, the effectiveness diminishes because of the directing loss of the diodes and the resistance loss of the capacitors. The most astounding framework proficiency for these three data voltages shows up at yield power (Po) load. A most extreme 93.15% effectiveness is accomplished at 48 V data voltage. At last, the hypothetical, recreated, and test voltage increases under Vin=48 V, RL=1 kω, fsc=1 kHz, fsm=60 kHz. Seven separate stages (n=1 to 7) of CW circuit were utilized, while the exploratory results show just for n=1 to 7. The proficiency of the proposed converter with diverse data voltages are 42V, 48V and 54V. The yield voltage of the proposed converter is controlled at 1.05kV, subsequently, the voltage additions relating to these three information voltages are 10.7, 9.4 and 8.3, separately. The recreation of yield current waveform is demonstrated in figure 9. The outcomes speak to that the proposed converter has lower effectiveness at lower info due to higher leading misfortune joined by higher data current. Then again, for higher burden condition, the proficiency diminishes because of the leading loss of the diodes and the resistance loss of the capacitors. The most noteworthy framework proficiency for these three info voltages shows up at depends load. A greatest 93.15% productivity is attained to at 54V information voltage. The reason is that the impact of the parasitic components increments when the proposed converter works under high obligation cycle, and the voltage addition will be decayed. The proposed converter still can give high voltage pick up without great high obligation cycle. Accordingly the reproduction of the DC-DC help converter utilizing Cockcroft Walton voltage multiplier was effectively done utilizing MATLAB simulink programming and the yield waveforms were watched.

Fig.16: *Few Significant Points Regarding the Power Circuit*

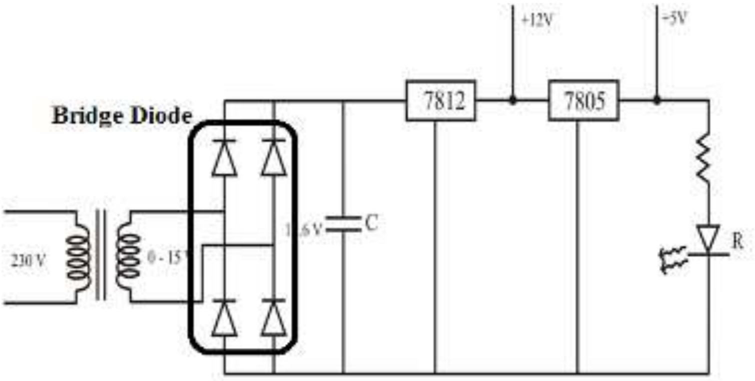

A stage down transformer (230/15) V is utilized to give include supply to the force circuit. The 15V air conditioner data is amended into 15V throbbing DC with the assistance of full extension rectifier circuit. The swells in the throbbing DC are uprooted and unadulterated DC is acquired by utilizing a capacitor filter. The positive terminal of the capacitor is joined with the data pin of the 7812 controller for voltage regulation. A yield voltage of 12V got from the yield pin of 7812 is encouraged as the supply to the beat amplifier. An yield voltage of 5V acquired from the yield pin of 7805 is sustained as the supply to the micro controller. From the same yield pin of the 7805, a Drove is associated in arrangement with the resistor to demonstrate that the force is ON.

CONCLUSION

In this paper subsequent to the voltage weight on the dynamic switches, diodes, and capacitors is not influenced by the quantity of fell stages, power segments with same voltage appraisals can be chosen. The scientific displaying, circuit operation, plan contemplations, and control method were talked about. The control method of the proposed converter can be effectively actualized with a business normal current-control and nonstop current mode with including a customized. The proposed control methodology utilizes two autonomous frequencies, one of which works at high recurrence to minimize the span of the inductor, while the other one works at moderately low recurrence as indicated by the sought yield voltage swell. At long last, the reproduction and test results demonstrated the legitimacy of hypothetical examination and the plausibility of the proposed converter.

REFERENCES

[1] J. P. Benner and L. Kazmerski, "Photovoltaics gaining greater visibility," *IEEE Spectr.*, vol. 36, no. 9, pp. 34–42, Sep. 1999.

[2] Z. Zhao, M. Xu, Q. Chen, J.-S. Lai, and Y. Cho, "Derivation of boost-buck converter based high-efficiency robust PV inverter," in *Proc. IEEE Energy Convers. Cong. Expos.*, Sep. 12–16, 2010, pp. 1479–1484.

[3] R. W. Erickson and A. P. Rogers, "A micro inverter for building-integrated photovoltaics," in *Proc. 24th Annu. IEEE Appl. Power Electron. Conf. Expos.*, Feb. 15–19, 2009, pp. 911–917.

[4] S. B. Kjaer, J. K. Pedersen, and F. Blaabjerg, "A review of single-phase grid-connected inverters for photovoltaic modules," IEEE *Trans. Ind. Appl.*, vol. 41, no. 5, pp. 1292–

1306, Sep./Oct. 2005.

[5] E. Koutroulis and F. Blaabjerg, “Design optimization of grid-connected PV inverters,” in *Proc. 26th Annu. IEEE Appl. Power Electron. Conf. Expos.*, Mar. 6–11, 2011, pp. 691–698.

[6] T. Kerekes, R. Teodorescu, P. Rodr´ıguez, G. Va´zquez, and E. Aldabas, “A new high-efficiency single-phase transformerless PV inverter topology,” *IEEE Trans. Ind. Electron.*, vol. 58, no. 1, pp. 184–191, Jan. 2011.

[7] O. Lopez, F. D. Freijedo, A. G. Yepes, P. Fernandez-Comesaa, J. Malvar, R. Teodorescu, and J. Doval-Gandoy, “Eliminating ground current in a transformerless photovoltaic application,” *IEEE Trans. Energy Convers.*, vol. 25, no. 1, pp. 140–147, Mar. 2010.

[8] E. Gub´ıa, P. Sanchis, A. Ursu´ a, J. Lopez, and L. Marroyo, “Ground currents in single-phase transformerless photovoltaic systems,” *Prog. Photovolt., Res. Appl.*, vol. 15, pp. 629–650, 2007.

[9] S. V. Araujo, P. Zacharias, and B. Sahan, “Novel grid-connected non- isolated converters for photovoltaic systems with grounded generator,” in *Proc. IEEE Power Electron. Spec. Conf.*, Jun. 15–19, 2008, pp. 58–65.

[10] B. Yang, W. Li, Y. Gu, W. Cui, and X. He, “Improved transformerless inverter with common-mode leakage current elimination for a photovoltaic grid-connected power system,” IEEE *Trans. Power Electron.*, vol. 27, no. 2, pp. 752–762, Feb. 2012.

[11] V. Matthias, G. Frank, B. Sven, and H. Uwe, German Patent H5-Topology, DE 102004030912 B3, Jan. 2006.

[12] S. Heribert, S. Christoph, and K. Juergen, German Patent HERIC - Topology, DE 10221592 A1, Apr. 2003.

[13] W. Yu, J.-S. Lai, H. Qian, C. Hutchens, J. Zhang, G. Lisi, A. Djabbari, G. Smith, and T. Hegarty, “High-efficiency inverter with H6-type config- uration for photovoltaic non-isolated ac module applications,” in *Proc. 25th Annu. IEEE Appl. Power Electron. Conf. Expos.*, Feb. 21–25, 2010, pp. 1056–1061.

[14] W. Cui, B. Yang, Y. Zhao, W. Li, and X. He, “A novel single-phase transformerless grid-connected inverter,” in *Proc. 37th Annu. Conf. IEEE Ind. Electron. Soc.*, Nov. 7–10, 2011, pp. 1126–1130.

[15] B. Yang, W. Li, Y. Deng, X. He, S. Lambert, and V. Pickert, “A novel single-phase transformerless photovoltaic inverter connected to grid,” in *Proc. 5th IET Int. Conf. Power Electron., Mach. Drives*, Apr. 19–21, 2010, pp. 1–6.

[16] R. Gonzalez, J. Lopez, P. Sanchis, E. Gubia, A. Ursua, and L. Marroyo, “High-efficiency transformerless single-phase photovoltaic inverter,” in *Proc. 12th Int. Power Electron. Motion Control Conf.*, Aug. 30–Sep. 1, 2006, pp. 1895–1900.

[17] R. Gonzalez, E. Gubia, J. Lopez, and L. Marroyo, “Transformerless single- phase multilevel-based photovoltaic inverter,” *IEEE Trans. Ind. Electron.*, vol. 55, no. 7, pp. 2694–2702, Jul. 2008.

[18] H. Xiao and S. Xie, “Transformerless split-inductor neutral point clamped three-level PV grid-connected inverter,” IEEE *Trans. Power Electron.*, vol. 27, no. 4, pp. 1799–1808, Apr. 2012.

[19] K. Dietrich, German Patent Wechselrichter: DE 19642522 C1, Apr. 1998.

[20] S. V. Araujo, P. Zacharias, and R. Mallwitz, “Highly efficient single-phase transformerless inverters for grid-connected photovoltaic systems,” *IEEE Trans. Ind.*

Electron., vol. 57, no. 9, pp. 3118–3128, Sep. 2010.

[21] D. Barater, G. Franceschini, and E. Lorenzani, “Unipolar PWM for trans- formerless grid-connected converters in photovoltaic plants,” in *Proc. Int. Conf. Clean Electr. Power*, Jun. 9–11, 2009, pp. 387–392.

[22] H. Xiao, S. Xie, Y. Chen, and R. Huang, “An optimized transformerless photovoltaic grid-connected inverter,” *IEEE Trans. Ind. Electron.*, vol. 58, no. 5, pp. 1887–1895, May 2011.

[23] T. Kerekes, R. Teodorescu, P. Rodr´ıguez, G. Va´zquez, and E. Aldabas, “A new high-efficiency single-phase transformerless PV inverter topology,” *IEEE Trans. Ind. Electron.*, vol. 58, no. 1, pp. 184–191, Jan. 2011.

[24] Y. Zhao, W. Li, Y. Deng, and X. He, “High step-up boost converter with passive lossless clamp circuit for non-isolated high step-up applications,” *IET Power Electron.*, vol. 4, no. 8, pp. 851–859, Sep. 2011.